Quantum mechanics predicts Bicoid interpretation times of less than a second

Irfan Lone*
Canadian Quantum Research Center, Ave Vernon, British Columbia 204-3002 32, Canada. and Indian Institute of Technology Bombay, Powai, Mumbai 400076, India.
(Dated: September 10, 2024)

The establishment and interpretation of the concentration distribution of the morphogen Bicoid (*Bcd*) is considered crucial for the successful embryonic development of fruit flies. However, the biophysical mechanisms behind the timely formation and subsequent interpretation of this prototypical morphogenetic system by its target genes are not yet completely understood. Recently a discrete time, one-dimensional quantum walk model of *Bcd* gradient formation has been successfully used to explain the observed multiple dynamic modes of the *Bcd* system. However, the question of its precise interpretation by its primary target gene hunchback (*hb*) remains still unanswered. In this paper it will be shown that the interpretation of the *Bcd* gradient by its primary target gene *hb*, with the observed precision of $\sim 10\%$, takes a time period of less than a second, as expected on the basis of recent experimental observations. Furthermore, the quantum walk model is also used to explain certain key observations of recent optogenetic experiments concerning the time windows for *Bcd* interpretation. Finally, it is concluded that the incorporation of quantum effects into the treatment of *Bcd* gradient represents a viable step in exploring the dynamics of morphogen gradients.

The establishment of concentration distributions of certain signalling molecules, commonly called morphogens, plays a key role during embryonic development of multi-cellular organisms [1–5]. For example, the concentration distribution of *Bcd* established during the early embryonic development of fruit flies provides the necessary positional information for the proper implementation of the body plan of the organism and has been studied in the greatest detail [6–10]. The timely establishment and precise interpretation of *Bcd* by its primary target gene *hb* is considered crucial for the successful development of the fly. Extracellular diffusion accompanied by a unimolecular first order degradation is thought to be the dominant mechanism behind the establishment of *Bcd* morphogen distribution in the fruit fly syncytium. Beginning with the classical Markovian model of morphogen gradient formation by Crick [11], the conventional random walk models of *Bcd* gradient formation [12–14] haven't yielded a completely satisfactory explanation of its underlying dynamics.

Most importantly, the biophysical mechanisms behind the precise interpretation of *Bcd* by its primary target gene *hb* remain still elusive [15–26]. Equilibrium models fail to capture this important aspect of the morphogen in a satisfactory manner and the formulation of increasingly more complex approaches has been suggested [19]. Theories employing detailed balance arguments have also not proven much helpful in this regard [27]. Recent theoretical treatments invoking hypotheses like dynamically changing time windows predict an interpretation time of less than a minute and remain unsubstantiated in vivo [22, 23, 28]. However, experimentally *Bcd* is known to bind to chromatin sites in a highly transient manner, with specific binding events lasting on the order of a second, in all portions of the embryo [20]. This demands interpretation times of duration less than a second. Thus, despite extensive numerical and analytical work, the problem of interpretation of the *Bcd* morphogen by its primary target gene *hb* still has no satisfactory solution.

In contrast, a recent experimental observation, utilising fluorescence correlation spectroscopy (FCS) and perturbative techniques, has revealed multiple modes of *Bcd* transport at different spatial and temporal locations across the embryo [29]. Exploring the different dynamic modes for *Bcd*, it has been observed that in the cytoplasm the slow dynamic mode is similar across the embryo while as the fast one shows an increased diffusivity from the anterior to the posterior side. Similarly, in the nuclei the *Bcd* diffusivity shows a significant, though comparatively small, increase in the fast dynamic mode from the anterior to the posterior regions, with the slow component remaining essentially unchanged [29].

These observations have been explained through a model fundamentally based on quantum mechanics [30]. This has been achieved by making use of an aspect of quantum information theory called a discrete time quantum walk (Fig. 1). A special case of the formalism for quantum Markov chains is a framework known as the quantum walk [31]. The quantum walk is a powerful generalization of random walk obtained by imposing quantum mechanics on the walker's dynamics and works in connection with diffusion in quantum dynamics, in particular, to model the dynamics of a quantum particle on a lattice. It has also garnered numerous applications in diverse areas from understanding the principles underlying various phenomena in physics, chemistry and biology to the designing of search algorithms for quantum computation [32–36]. However, quantum walks in actual physical systems differ from idealized models of quantum walks in several significant ways. Firstly, Hamiltonians of physical systems typically possess energy mismatches between sites leading to Anderson localization [37]. Secondly, actual quantum walks are subject to relatively high levels of environment-induced noise and decoherence.

Methods borrowed from quantum mechanics have been employed in the analysis of morphogen gradients previously as well. For example, the problem of time-dependent noise has been analyzed through the use of quantum-mechanical perturbation theory [38]. A Green's propagator,

$$G(x_1, x_2, \omega) = \int_0^\infty d\lambda \frac{\hat{\psi}_\lambda(x_1)\hat{\psi}_\lambda(x_2)}{-i\omega + \lambda}, \tag{1}$$

is constructed from the set of eigenfunctions $\hat{\psi}_\lambda$ of a linear operator $\partial_x^2 + 12/(x+\epsilon^2)$ in a non-linear reaction-diffusion model

$$\partial_t \delta\phi = \partial_x^2 \delta\phi - \frac{12}{(x+\epsilon)^2}\delta\phi - \delta\phi^2 + \delta\eta\delta\phi. \tag{2}$$

and the iterative solution to the problem, obtained by repeated substitution for the non-linear terms, is then expressed as a sum over tree Feynman diagrams [38]. In Eq. (2) $\phi(x,t)$ denotes the local concentration of morphogen that is produced at the origin at a variable rate η and diffuses out to infinity along the positive x axis with Fick's constant D accelerating its own degradation at a local rate $f\phi(x.t)^2$. Also

$$\epsilon = \frac{12D^2}{f\eta}^{1/3}, \tag{3}$$

and $\delta\eta(t)$ is the time-dependent noise that itself is taken to satisfy,

$$\langle \delta\eta(t) \rangle = 0, \tag{4}$$

and

$$\langle \delta\eta(t)\delta\eta(t') \rangle = 2\gamma\delta(t-t'), \tag{5}$$

the so-called white noise [39], where $\delta(t)$ and $\delta(t-t')$ denote the usual Dirac delta functions.

In a quantum walk treatment the degradation of *Bcd* is modelled as a unitary noise that is intrinsic and that does not cause any entanglement with the environment, such that the system remains in an essentially pure state during the course of its evolution [30]. It thus acts like a classical fluctuating field such that the dynamics of the system is unitary, yet stochastic [40]. Thus, the quantization of Bcd system accounts for its relaxation to a non-equilibrium steady-state. Now, the timescale of *Bcd* driven pattern formation in the fly embryo can be divided into two sub-intervals. First 90 minutes, prior to nuclear cycle 10, are utilised by the system for the establishment of the *Bcd* gradient in the embryo [41]. From nuclear cycle 10 onward the *Bcd* concentration inside the nuclei remains stable from cycle to cycle. The quantitative relationship between the statistics of *hb* expression levels is consistent with a model in which the dominant source of noise are the diffusive fluctuations associated with the random arrival of *Bcd* molecules at their target sites [42].

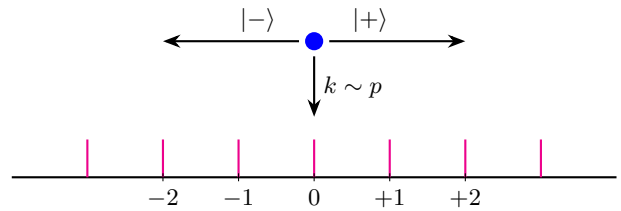

FIG. 1. Schematic of the quantum walk model. Bcd molecule (shown by the blue colored dot) can, respectively, make a transition to the right or to the left depending on its chirality state of $|+\rangle$ or $|-\rangle$ or it can get degraded at a rate k.

This noise is quantitatively expressed by the Berg-Purcell limit,

$$\frac{\delta\phi}{\phi} \sim \frac{1}{\sqrt{Da\phi T}}, \tag{6}$$

in which a denotes the size of the *Bcd* receptor and T is the duration of signal integration [43].

Intriguingly, what Gregor *et al.* discovered is that the observed precision of $\sim 10\%$ in the readout of the *Bcd* concentration by the nuclei is inconsistent with the predictions of this fundamental physical limit for diffusive processes [15]. To circumvent this problem, the idea of spatial averaging by the nuclei was introduced by the authors in order to increase the precision to the desired level [15]. Over the years the mechanism of Gregor *et al.* has been widely applied [16–19, 44, 45] but the problem of interpretation of *Bcd* gradient by its primary target gene *hb* still remains poorly understood [19–28]. In fact a recent theoretical analysis has shown that spatial averaging is *a priori* dispensable but the treatment introduces another *ad hoc* hypothesis of dynamically changing time windows [28]. Most importantly, it predicts an interpretation time much higher than is supported by current experimental observations based on lattice light sheet microscopy studies [20].

In this Letter we employ the quantum walk model to show that it can successfully explain the precise interpretation of the *Bcd* morphogen by its target genes [15] and certain key observations of recent optogenetic experiments concerning the time windows for *Bcd* interpretation are also readily explained by the said model [46].

From the quantum walk based treatment [30], one obtains the following set of four quantum-classical master equations for the formation of the the *Bcd* gradient:

$$P_n(t+1) = \frac{1}{2}P_{n+1}(t) + \frac{1}{2}P_{n-1}(t) + \sigma_{n+1}(t) - \sigma_{n-1}(t),$$

$$P_n(t+1) = \frac{1}{2}P_{n-1}(t) + \frac{1}{2}P_n(t) - \sigma_{n-1}(t) - \sigma_n(t),$$

$$P_n(t+1) = \frac{1}{2}P_n(t) + \frac{1}{2}P_{n+1}(t) + \sigma_n(t) + \sigma_{n+1}(t),$$

$$P_n(t+1) = P_n(t). \tag{7}$$

with the occupation probabilities $P_n(t)$ representing the classical part and the coherence (σ) terms the non-classical contribution, where $\sigma \equiv \Re[a^{+*}a^{-}]$ and the symbol $\Re$ stands for the real part. If we ignore the σ terms and combine the resulting expressions into one single equation then a straightforward scaling argument gives the following result,

$$P_n(t+1) = P_n(t) + \frac{1}{2}(1-p)P_{n+1}(t) + \frac{1}{2}(1-p)P_{n-1}(t),$$

which yields the following diffusion equation

$$\partial_t P(x,t) = D'\partial_x^2 P(x,t), \tag{8}$$

with the diffusion constant defined as

$$D' = \frac{1}{2}(1-p), \tag{9}$$

where we have explicitly switched to continuous position and time variables (x, t) in arriving at Eq. (8). Solution of the above set of quantum-classical equations, Eqs. (7), without neglecting the coherence (σ) terms gives the following expression for the diffusion constant of the system

$$D = \frac{A(1-p)}{p}, \tag{10}$$

where p is a parameter that quantifies noise in the system and the coefficient A is a function of p with an estimated value of ~ 0.40 and $A \to 0.5$ as $p \to 1$ [30]. Remarkably, Crick, using his source-sink model,

$$D = \frac{A(Nl)^2}{t}, \tag{11}$$

has estimated a value of $A = 0.42$ and proposed a general value of $A = 0.5$ for the biochemically more realistic models; where t is time, N is number of cells between source and sink, and l is length of each cell [11]. As per Eq. (10), the dominant contribution to the diffusion coefficient depends inversely on noise. Based on the currently available values of diffusivity, which are measured around nuclear cycle 14, *Bcd* is classified as a mid-range morphogen [47]. However, recent work has detected significant concentration of *Bcd* in the posterior-most parts of the embryo. For example, lattice light sheet microscopy studies have revealed highly dynamic *Bcd* molecules in the posterior end of the embryo with a diffusive-like kinetic behavior [20]. With the observed low levels of degradation, and hence noise, that are known in the literature [48] the possible values of diffusivity for *Bcd* as per Eq. (10) can be an order of magnitude higher than are currently known (see Fig. 2). Such large diffusion coefficients for morphogens are not an uncommon occurrence and values as high as $50 - 80\mu m^2 s^{-1}$ have been measured in different cellular contexts [47]. Lower noise rates, especially in earlier nuclear cycles, will yield very large diffusion coefficients for the system. Most quantitative studies of fruit fly development have, however, focused on nuclear cycle 14 embryos where the nuclei are easily accessible for imaging [9].

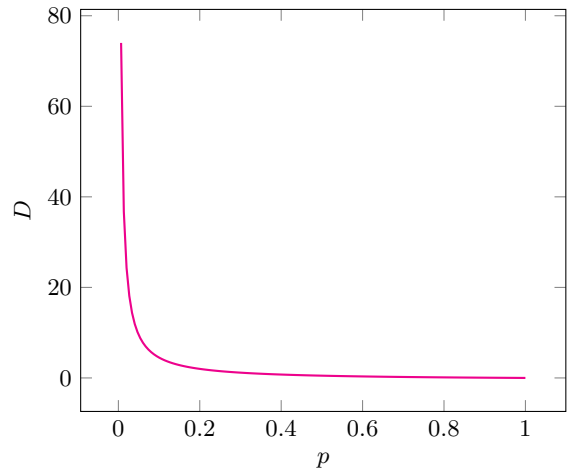

FIG. 2. Plot of Eq. (10), as a function of noise, p. The magnitude of D is large for very small p.

A very high diffusion rate predicted by above model and confirmed experimentally can also solve the problem of generating an appropriate gradient sufficiently fast for significantly larger patterning fields and *Bcd* could also become classified as a long-range morphogen like Nodal, Lefty and FGF8 in the zebrafish embryo [47]. Thus, as per the quantum walk model there is no single characteristic value of local diffusivity for the *Bcd* system but a range of possible values and the high values of *Bcd* diffusivity obtained through FCS measurements [29] are a consequence of Eq. (10). Furthermore, higher and higher values of diffusivity should be expected when the noise levels are very small especially in early nuclear cycles. It is pertinent to mention here that an analysis based on protein lifetime measurements has shown that a temporally varying diffusivity for *Bcd* is somewhat better at capturing the dynamics of gradient formation for this morphogen compared to the conventional treatments that assume a constant diffusion rate [49]. However, the precise mechanism behind such temporal dependence remains unknown [49]. The quantum walk model provides an explanation of this observation by showing that if the system can vary its diffusivity depending upon its requirement by modulating noise, then there is no single fixed value of local diffusivity for the system but rather a range of possible values. What this means, in other words, is that the *Bcd* protein mobility changes with time and spatial position in the embryo as is found experimentally to be the case as well [29].

Using florescence correlation spectroscopy (FCS) combined with certain perturbative techniques, Athilingam

et al. [29] have demonstrated that a two-component fit to the FCS curves is substantially better than a one-component fit in both the cytoplasm and nucleus, implying the presence of two dynamic modes in each region. There are thus, at least, four effective modes of Bcd transport: (1) fast cytoplasmic mode, (2) slow cytoplasmic mode, (3) fast nuclear localised mode, and (4) slow nuclear localised mode. The effective diffusion coefficient,

$$D_{eff} = g_f D_f + g_s D_s, \tag{12}$$

increases from the anterior to the posterior side of the embryo; where D_f, D_s and g_f, g_s represent the diffusion coefficients and fractions for the fast and slow dynamic modes, respectively, with

$$g_f + g_s = 1. \tag{13}$$

Clearly, in the quantum walk model D_s and D_f correspond, respectively, to D' and D from Eqs. (9) and (10). Therefore, the expression for the effective diffusivity of the system may also be expressed as

$$D_{eff} = g_f \frac{A(1-p)}{p} + g_s \frac{1}{2}(1-p). \tag{14}$$

Equation (14) has recently been used to explain the origin of the multiple dynamic modes that accompany the formation of the *Bcd* gradient in the early fruit fly embryogenesis [30]. Here we shall use them to explain the *Bcd* interpretation time by its primary target genes.

Now, as per the quantum walk model the diffusivity of *Bcd*, Eq. (10), is very large for the observed low noise levels in the system and the system can vary its diffusivity depending upon its requirement by modulating noise [30]. It is thus quite conceivable that a significant fraction of *Bcd* molecules can move much faster given the very low observed degradation rates ($k \sim 10^{-4}s^{-1}$) of the *Bcd* morphogen in the system [48]. It seems that the system has evolved in such a way as to keep the degradation, and hence noise levels, under control around low values. This has developmental advantage since higher noise rates would mean lower diffusivity, Eq. (10), and therefore less and less moprhogen reaching a given location in the tissue, thus compromising the consequent transfer of positional information [30]. Substituting Eq. (10) in Eq. (6) one obtains

$$\frac{\delta\phi}{\phi} \sim \sqrt{\frac{p}{A(1-p)a\phi T}}, \tag{15}$$

Equation (15) is our modified Berg-Purcell limit for the *Bcd* gradient. We now use Eq. (15) to explain how *Bcd* gradient can be precisely decoded by its primary target gene *hb* as follows. For the numerical values of noise p comparable in magnitude to the observed *Bcd* degradation rates ($k \sim 10^{-4}s^{-1}$) in the system, and substituting the values of concentration ϕ and receptor size a from [15] into Eq. (15)

$$\frac{\delta\phi}{\phi} \sim \left[\frac{0.5(1-0.0001)\mu m^2 s^{-1} 3nm \times 4.8\mu m^{-3} T}{0.0001}\right]^{-1/2}$$

shows that the decoding of positional information from the *Bcd* morphogen by its primary target gene *hb*, with the observed precision of $\sim 10\%$ ($\delta\phi/\phi \sim 0.1$) takes $T \sim 0.7s$, which is less than a second. From this one can readily calculate the on-rate of the *Bcd* morphogen for its target loci,

$$k_{on} \sim T^{-1} \sim 1.43s^{-1},$$

which is a very moderate on-rate. This is significant considering that lattice light sheet microscopy experiments have shown *Bcd* binding to chromatin sites in a highly transient manner, with specific binding events lasting on the order of a second, in all portions of the embryo with a rapid off rate such that its average occupancy at target loci is on-rate dependent [20].

We shall now briefly explain the observed time windows for *Bcd* interpretation. By subjecting the fly embryos to illumination at precisely defined stages, distinct time windows for the interpretation of *Bcd* have been defined through optogenetic experiments [46]. It has been demonstrated that temporal integration is indeed a necessary process in *Bcd* decoding with the integration time window covering as long as 90 minutes from nuclear cycle 10 until the end of nuclear cycle 14 [46]. Interestingly, the nuclei exposed to highest local *Bcd* concentration, those on the anterior side, integrated the signal for the longest duration while those receiving lower *Bcd* dosage, that is nuclei closer to the posterior side, required the inputs for comparatively shorter times in order to arrive at correct cell fates [46]. Now, a spatio-temporally nonuniform degradation of *Bcd* could lead to a non-uniform distribution of noise in the system. This non-uniformity is due to the higher concentration of *Bcd* on the anterior side of the embryo than that towards the posterior side. This is despite the fact that the net concentration of *Bcd* inside the nuclei at a given position along the AP-axis remains constant within $\sim 10\%$ accuracy from nuclear cycle 10 onward [41]. The net effect of all these increased noise processes on the anterior is to reduce the diffusivity of the system, the $A(1-p)/p$ term in Eq. (15), more on the anterior side and consequently the nuclei on this side need to integrate the signal for a longer duration, higher T values, in order to reach the desired level ($\sim 10\%$) of precision in signal interpretation. Hence the resulting differing time windows.

The above discussion focused on a very simple model of *Bcd* gradient formation and its subsequent interpretation by the nuclei. The environment in which the *Bcd* gradient forms is highly dynamic and heterogeneous. In fact, the Markovian behavior is always an idealization

in the description of the dynamics of open systems with non-Markovianity being non-negligible in a number of different scenarios especially biological [50]. However, the system we dealt with in this work is unique and special in so many ways that even a Markovian description suffices. The *Bcd* system is essentially a one-dimensional problem since patterning systems along different axes of the embryo are independent of each other [51]. Hence a simple one-dimensional quantum walk treatment becomes possible. It would be interesting to see whether a similar type of analysis can be carried out for other morphogens, particularly the gradient of the morphogen *Dpp* established orthogonal to *Bcd* along the dorso-ventral axis of the embryo [52]. Despite the apparent simplicity of above approach it makes, in addition to explaining the observed features of the system, certain new and useful predictions. Most importantly, as is clear from Eq. (15), we find that the problems of gradient formation and interpretation are interconnected processes, at least in the case of *Bcd* system. In this regard above model is a very rare instance of a long desired approach [53] that incorporates both the dynamics of morphogen gradient formation and its subsequent interpretation. Specifically, we find that the embryo does not need to rely on complex mechanisms like spatial averaging [16] and dynamically changing time windows [28] in order to generate precise boundaries of gene expression in a short span of time. Rather, the very large values of diffusivity attained by the system are sufficient to achieve the desired level of precision in the patterning processes.

In conclusion we have used the recently proposed quantum walk model of *Bcd* gradient formation to explain the precise interpretation of the *Bcd* morphogen by its primary target gene *hb* with the observed precision of $\sim 10\%$ [15] and certain key observations of recent optogenetic experiments concerning the time windows for *Bcd* interpretation are also readily explained by the said model [46]. It is found that the very large values of diffusivity are responsible for generating precise boundaries of gene expression in a short span of time. This is in contrast to the conventional treatments that require complex mechanisms like spatial averaging and dynamically changing time windows to achieve the desired level of precision in the patterning processes. This demonstrates that the incorporation of quantum effects into the dynamics of *Bcd* gradient formation and interpretation represents a viable step forward in exploring the biophysics of this prototypical morphogen, and perhaps other morphogens like the *Dpp* gradient in the developing fly wing [52], in light of recent experimental observations on the system.

I would like to thank Carl Trindle for financial support.

* Correspondence.
loneirfan@iitb.ac.in

[1] A. Kicheva and J. Briscoe, Annu. Rev. Cell Dev. Biol. **39**, 91 (2023).
[2] M. F. Simsek and E. M. Özbudak, Open Biol. **12**, 220224 (2022).
[3] K. S. Stapornwongkul and J.-P. Vincent, Nat. Rev. Genet. **22**, 393 (2021).
[4] L. Wolpert, J. Theor. Biol. **25**, 1 (1969).
[5] A. M. Berezhkovskii, C. Sample, and S. Y. Shvartsman, Biophys. J. **99**, L59 (2010).
[6] W. Driever and C. Nüsslein-Volhard, Cell **54**, 83 (1988); **54**, 95 (1988).
[7] A. Ephrussi and D. St Johnston, Cell **116**, 143 (2004).
[8] O. Crauk and N. Dostatni, Curr. Biol. **15**, 1888 (2005).
[9] A. Huang and T. E. Saunders, Curr. Top. Dev. Biol. **137**, 79 (2020).
[10] A. P. Singh, P. Wu, S. Ryabichko, J. Raimundo, M. Swan, E. Wieschaus, T. Gregor, and J. E. Toettcher, Cell Rep. **38** (2022).
[11] F. Crick, Nature **225**, 420 (1970).
[12] O. Grimm, M. Coppey, and E. Wieschaus, Development **137**, 2253 (2010).
[13] H. Teimouri and A. B. Kolomeisky, J. Phys. A: Math. Theor. **49**, 483001 (2016).
[14] G. Schlissel, M. Meziane, D. Narducci, A. S. Hansen, and P. Li, Proc. Natl. Acad. Sci. U. S. A. **121**, e2400677121 (2024).
[15] T. Gregor, D. W. Tank, E. F. Wieschaus, and W. Bialek, Cell **130**, 153 (2007).
[16] T. Erdmann, M. Howard, and P. R. Ten Wolde, Phys. Rev. Lett. **103**, 258101 (2009).
[17] A. Porcher, A. Abu-Arish, S. Huart, B. Roelens, C. Fradin, and N. Dostatni, Development **137**, 2795 (2010).
[18] S. C. Little, M. Tikhonov, and T. Gregor, Cell **154**, 789 (2013).
[19] T. Lucas, H. Tran, C. A. Perez Romero, A. Guillou, C. Fradin, M. Coppey, A. M. Walczak, and N. Dostatni, PLoS genetics **14**, e1007676 (2018).
[20] M. Mir, A. Reimer, J. E. Haines, X.-Y. Li, M. Stadler, H. Garcia, M. B. Eisen, and X. Darzacq, Genes & Dev. **31**, 1784 (2017).
[21] H. Tran, A. M. Walczak, and N. Dostatni, Curr. Top. Dev. Biol. **137**, 119 (2020).
[22] Y. Song and C. Hyeon, Elife **10**, e70034 (2021).
[23] G. Fernandes, H. Tran, M. Andrieu, Y. Diaw, C. P. Romero, C. Fradin, M. Coppey, A. M. Walczak, and N. Dostatni, Elife **11**, e74509 (2022).
[24] D. Iber and R. Vetter, Current Opinion in Genetics & Development **75**, 101916 (2022).
[25] S. Baumgartner, Hereditas **161**, 1 (2024).
[26] L. Zhang, L. Hodgins, S. Sakib, A. Verbeem, A. Mahmood, C. Perez-Romero, R. A. Marmion, N. Dostatni, and C. Fradin, Biophys. J (2024).
[27] J. Estrada, F. Wong, A. DePace, and J. Gunawardena, Cell **166**, 234 (2016).
[28] J. Desponds, M. Vergassola, and A. M. Walczak, Elife **9**, e49758 (2020).
[29] T. Athilingam, A. V. Nelanuthala, C. Breen, N. Karedla, M. Fritzsche, T. Wohland, and T. E. Saunders, Develop-

ment **151** (2024).
[30] I. Lone and C. O. Trindle, AIP Advances **14** (2024).
[31] S. Gudder, J. Math. Phys. **49**, 072105 (2008).
[32] N. Shenvi, J. Kempe, and K. B. Whaley, Phys. Rev. A **67**, 052307 (2003).
[33] M. Mohseni, P. Rebentrost, S. Lloyd, and A. Aspuru-Guzik, J. Chem. Phys. **129** (2008).
[34] O. Mülken and A. Blumen, Phys. Rep. **502**, 37 (2011).
[35] A. Chia, K. Tan, Ł. Pawela, P. Kurzyński, T. Paterek, and D. Kaszlikowski, Phys. Rev. E **93**, 032407 (2016).
[36] N. B. Lovett, S. Cooper, M. Everitt, M. Trevers, and V. Kendon, Phys. Rev. A **81**, 042330 (2010).
[37] P. W. Anderson, Phys. Rev. **109**, 1492 (1958).
[38] J. L. England and J. Cardy, Phys. Rev. Lett. **94**, 078101 (2005).
[39] C. Gardiner, *Stochastic methods*, 4th ed. (Springer Berlin Heidelberg, 2009).
[40] Since the unitary noise in the Bcd system is intrinsic and does not cause any entanglement with the environment such that the system remains in an essentially pure state during the course of its evolution, the system can be treated as a closed one for all practical purposes. This is especially true for very early nuclear cycles [12].
[41] T. Gregor, E. F. Wieschaus, A. P. McGregor, W. Bialek, and D. W. Tank, Cell **130**, 141 (2007).
[42] G. Tkačik, T. Gregor, and W. Bialek, PloS One **3**, e2774 (2008).
[43] W. Bialek and S. Setayeshgar, Proc. Natl. Acad. Sci. USA **102**, 10040 (2005).
[44] A. Ochoa-Espinosa, D. Yu, A. Tsirigos, P. Struffi, and S. Small, Proc. Natl. Acad. Sci. U. S. A. **106**, 3823 (2009).
[45] Y. Okabe-Oho, H. Murakami, S. Oho, and M. Sasai, PLoS Comput. Biol. **5**, e1000486 (2009).
[46] A. Huang, C. Amourda, S. Zhang, N. S. Tolwinski, and T. E. Saunders, Elife **6**, e26258 (2017).
[47] P. Müller, K. W. Rogers, S. R. Yu, M. Brand, and A. F. Schier, Development **140**, 1621 (2013).
[48] J. A. Drocco, O. Grimm, D. W. Tank, and E. Wieschaus, Biophys. J **101**, 1807 (2011).
[49] L. Durrieu, D. Kirrmaier, T. Schneidt, I. Kats, S. Raghavan, L. Hufnagel, T. E. Saunders, and M. Knop, Mol. Syst. Biol. **14**, e8355 (2018).
[50] H.-B. Chen, N. Lambert, Y.-C. Cheng, Y.-N. Chen, and F. Nori, Sci. Rep. **5**, 12753 (2015).
[51] J. Jaeger, Mol. BioSyst. **5**, 1549 (2009).
[52] A. Eldar, R. Dorfman, D. Weiss, H. Ashe, B.-Z. Shilo, and N. Barkai, Nature **419**, 304 (2002).
[53] P.-F. Lenne, E. Munro, I. Heemskerk, A. Warmflash, L. Bocanegra-Moreno, K. Kishi, A. Kicheva, Y. Long, A. Fruleux, A. Boudaoud, *et al.*, Phys. Biol. **18**, 041501 (2021).